



ELSEVIER

Design and characterization of two-dye and three-dye binary fluorescent probes for mRNA detection

Angel A. Martí,^a Xiaoxu Li,^c Steffen Jockusch,^a Nathan Stevens,^a Zengmin Li,^{b,c}
Bindu Raveendra,^c Sergey Kalachikov,^c Irina Morozova,^c James J. Russo,^c Daniel L. Akins,^d
Jingyue Ju^{b,c,*} and Nicholas J. Turro^{a,b,*}

^aDepartment of Chemistry, Columbia University, 3000 Broadway, New York, NY 10027, USA

^bDepartment of Chemical Engineering, Columbia University, 3000 Broadway, New York, NY 10027, USA

^cColumbia Genome Center, Columbia University College of Physicians and Surgeons, New York, NY 10032, USA

^dDepartment of Chemistry, City College, City University of New York, NY 10031, USA

Received 26 July 2006; revised 28 August 2006; accepted 28 August 2006

Available online 7 February 2007

Abstract—We report the design, synthesis, and characterization of binary oligonucleotide probes for mRNA detection. The probes were designed to avoid common problems found in standard binary probes such as direct excitation of the acceptor fluorophore and overlap between the donor and acceptor emission spectra. Two different probes were constructed that contained an array of either two or three dyes and were characterized using steady-state fluorescence spectroscopy, time-resolved fluorescence spectroscopy, and fluorescence depolarization measurements. The three-dye binary probe (**BP-3d**) consists of a Fam fluorophore which acts as a donor, collecting light and transferring it as energy to Tamra, which subsequently transfers energy to Cy5 when the two probes are hybridized to mRNA. This design allows the use of 488 nm excitation, which avoids the direct excitation of Cy5 and at the same time provides a good fluorescence resonance energy transfer (FRET) efficiency. The two-dye binary probe system (**BP-2d**) was constructed with Alexa488 and Cy5 fluorophores. Although the overlap between the fluorescence of Alexa488 and the absorption of Cy5 is relatively low, FRET still occurs due to their close physical proximity when the probes are hybridized to mRNA. This framework also decreases the direct excitation of Cy5 and reduces the fluorescence overlap between the donor and the acceptor. Picosecond time-resolved spectroscopy showed a reduction in the fluorescence lifetime of donor fluorophores after the formation of the hybrid between the probes and target mRNA. Interestingly, **BP-2d** in the presence of mRNA shows a slow rise in the fluorescence decay of Cy5 due to a relatively slow FRET rate, which together with the reduction in the Alexa488 lifetime provides a way to improve the signal to background ratio using time-resolved fluorescence spectra (TRES). In addition, fluorescence depolarization measurements showed complete depolarization of the acceptor dyes (Cy5) for both **BP-3d** (due to sequential FRET steps) and **BP-2d** (due to the relatively low FRET rate) in the presence of the mRNA target.

© 2007 Elsevier Ltd. All rights reserved.

1. Introduction

The elucidation of the human genome at the beginning of this century opened the door to new possibilities for treatment and diagnosis of disease,¹ a better understanding of memory and behaviors,^{2,3} and the study of our genetic evolution as a species,⁴ among other important, little understood areas of study. However, this achievement also poses a challenge for the development of new and improved methods for the detection and monitoring of DNA or RNA either in vitro or in vivo. Different approaches have been taken in the

design of oligonucleotide probes for DNA and RNA detection including molecular beacons (MBs),^{5–8} binary probes (BPs),^{9–13} and quenched autoligation probe pairs (QUAL).^{14–16} Other probes like scorpion primers,¹⁷ 5'-nuclease probes,¹⁸ and cyclicons¹⁹ have been used in vitro to detect amplification products in polymerase chain reactions (PCR). The versatility of these probes has made them the focus of intense research in the last few years.¹⁰

An MB is an oligonucleotide probe that forms a stem-loop structure in the absence of its target sequence (Fig. 1a).⁵ This probe possesses a fluorophore and a quencher attached at different ends of the oligonucleotide so that in the absence of target, the fluorophore and the quencher are in close proximity due to the formation of the stem-loop structure, and fluorescence is quenched. On the other hand, hybridization of the target sequence with the loop part of the MB promotes

Keywords: Binary probes; Fluorescence; Energy transfer; FRET; Time-resolved emission spectra (TRES); Cy5; Alexa488; Fam; Tamra; mRNA.

* Corresponding authors. Tel.: +1 212 851 5172; fax: +1 212 851 5176 (J.J.); tel.: +1 212 854 2175; fax: +1 212 932 1289 (N.J.T.); e-mail addresses: dj222@columbia.edu; njt3@columbia.edu

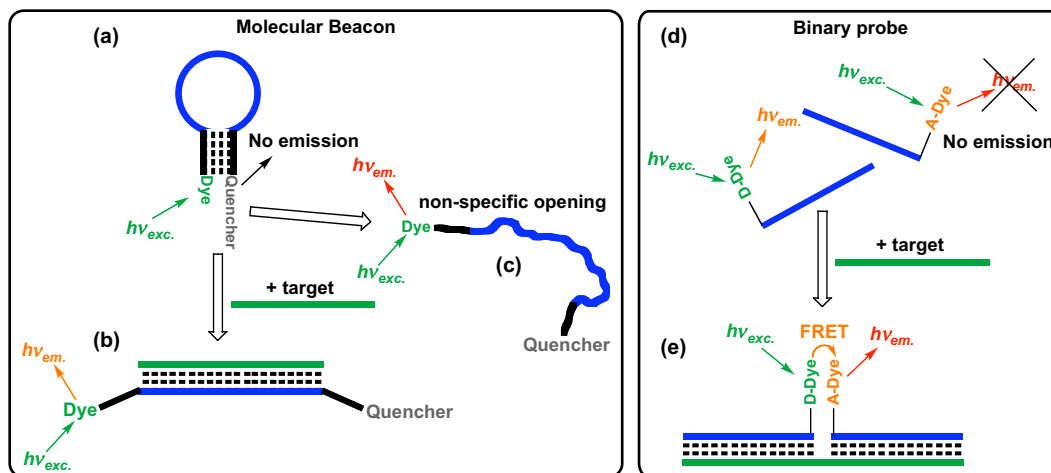


Figure 1. Molecular beacon in its 'closed' conformation before the addition of target (a), in the 'open' conformation after hybridization with target (b), and non-specific opening of the MB in the absence of target (c). Binary probes in the absence of target (d) and after hybridizing with target (e).

the formation of the double stranded helix and spatial separation of the fluorophore and the quencher, leading to the emission of fluorescence (Fig. 1b). (In an alternative MB design, different dyes rather than dye–quencher pairs can be used; excitation of the donor dye will lead to donor specific fluorescence in the absence, and FRET-induced acceptor emission in the presence of target mRNA.) MBs have several advantages such as high signal to background ratio (S/B),^{5,22,23} and fast hybridization response to complementary target,²⁴ which have been exploited for the detection of single nucleotide polymorphisms (SNPs).^{20,21} However, a notable disadvantage is non-specific opening of the MB (opening of the MB in the absence of target), which gives rise to a false positive signal (Fig. 1c).²⁵ Non-specific opening is a particular problem when MBs are used for mRNA imaging in living cells because of the many biological components of the cell (e.g., proteins) that are capable of complexing with and opening the MBs.²⁶

BPs, like MBs, are hybridization probes, but instead of having a single probe sequence, they are composed of two independent probe sequences, each with a fluorophore molecule, that are brought together upon hybridization with adjacent sections of the target (Fig. 1d).⁹ BPs rely mostly on FRET for target detection.^{9–12} In general, one of the sequences in the BP contains a donor fluorophore, while the second sequence should have an acceptor fluorophore, as shown schematically in Figure 1d. In the absence of the target, the probes are dispersed in solution and no FRET is observed. The presence of target causes hybridization of both probes to the target, which places the fluorophores into close proximity to one another. In this case, excitation of the donor fluorophore results in FRET to the acceptor fluorophore, producing the characteristic fluorescence signal of the acceptor. An ideal BP will show strong donor fluorescence and little or no acceptor fluorescence in the absence of target; the converse is expected when the target is present.¹¹ These conditions are generally fulfilled when there is no light absorption by the acceptor at the donor excitation wavelength, when the distance between the fluorophores is optimal, and when there is a good overlap between the donor fluorescence spectrum and the acceptor absorption spectrum.²⁷ One of the advantages of BPs is their high specificity since two

distinct probes must bind the target to produce the characteristic detection signal. BPs avoid false positive signals due to non-specific opening since the fluorescent detection signal occurs only when the probes are brought together, and this occurs only when both probes are specifically hybridized with the target.²⁸ Some potential applications of BPs include in vitro monitoring of RNA transcription,¹² cellular imaging,²⁷ and identification of gene translocation.¹¹ Nevertheless, there is still much room for improvement in the design of BPs. For example, BPs present relatively slow hybridization kinetics, since two probes must hybridize to the target for the signal to be detected.²⁹ Also, organic dyes present small Stokes' shifts, which usually produce an overlap between the donor and acceptor fluorescence spectra, decreasing the fluorescence contrast ratio (sensitivity) between the target-hybridized and free states.²⁸ Likewise, most of the acceptors possess finite absorption at the donor excitation, decreasing the fluorescence contrast ratio.³⁰

Rosmarin et al.²⁹ proposed an interesting solution to the slow hybridization kinetics of BPs. In their design called 'C' probes, they bind the two BP sequences with a linker, which does not interact with the target oligonucleotide but maintain the probes at a relatively close distance. Hybridization of one of the probe sequences to the target prompts the other one to hybridize rapidly to the target due to its close proximity. This has some additional advantages, such as better stability of the probe–target hybrid, due to a lesser loss of entropy after hybridization, and the handling of a single probe instead of two different ones.²⁹

Solutions to problems associated with the direct excitation of the acceptor fluorophore and small spectral overlap between the donor absorption and the acceptor emission require creative and novel approaches. We previously showed that a central fluorophore of a three-dye system can be used as an 'energy bridge' between a donor and an acceptor dye, allowing an increase in the separation of the donor absorption and the acceptor emission.³¹ In this design the donor used was 6-carboxyfluorescein (Fam), which after excitation transferred its energy to a rhodamine derivative, which functions as the primary acceptor/secondary donor, and subsequently transfers its energy to Cy5, the secondary acceptor.

This energy transfer cascade, similar in concept to that occurring in photosynthetic pathways, allows the efficient transfer of energy from Fam to a Cyanine-5 derivative (Cy5) using *N,N,N',N'*-tetramethyl-6-carboxyrhodamine derivative (Tamra) as an energy relay. Another important conclusion from this work was that systems containing just Fam and Cy5 still present considerable FRET ($\phi_{\text{FRET}}=0.43$).³¹ At first glance, this FRET efficiency may appear non-intuitive since the overlap between the donor fluorescence emission (Fam) and acceptor absorption spectrum (Cy5) appears to be very low. Nevertheless, Förster's theory of energy transfer indicates that a major factor affecting FRET between any two dyes is the distance between them;³² under Förster's paradigm the rate constant for FRET is directly proportional to the inverse sixth power of the distance between the dyes, while it is only linearly proportional with respect to the spectral overlap integral.³³ This suggests that even if the overlap integral is not substantial, a small distance between the fluorophores will lead to FRET occurring with significant efficiency. The advantage of the large spectral separation of the donor and acceptor dyes is the minimization of the excitation light absorption by the acceptor dye, which decreases the interfering background fluorescence in the absence of target.

In this manuscript, we explore two possibilities for the improvement of BP design: a three-dye system (**BP-3d**) with an intermediate fluorophore functioning as an energy relay in order to increase the amount of energy transferred to the final acceptor, and a two-dye system (**BP-2d**) in which the donor and acceptor present a poor spectral overlap but after hybridization with target the fluorophores are at a very close molecular distance. Different spectroscopic techniques, such as steady-state fluorescence spectroscopy, fluorescence depolarization, and picosecond time-resolved spectroscopy were employed with the purpose of evaluating the advantages and disadvantages of these approaches.

2. Materials and methods

2'-Methoxy RNA was synthesized on a DNA Synthesizer (Expedite 8909, Applied Biosystems, CA) by phosphoramidite chemistry using a set of 2'-OMe A^{bz}, G^{dmf}, C^{bz}, and U-CE phosphoramidite nucleosides (Glen Research, Sterling, VA). For donor probe synthesis, 3'-amino-modifier C3 CPG was used to generate 3'-amino-derived oligonucleotides; both 3'-amino-modifier C3 CPG and fluorescein-dT phosphoramidite were used to generate FAM labeled oligonucleotides bearing a free amino group at the 3' end. Cleavage and deprotection were carried out under mild conditions (concentrated NH₄OH at 40 °C, 17 h). The crude RNAs were obtained as a white solid after oligo purification cartridge (OPC) desalting (Applied Biosystems, CA) and drying. 3'-Amino RNA probes were coupled with Alexa488 NHS ester and FAM labeled 3'-amino RNA probes were further coupled with Tamra NHS ester in DMSO–0.1 M NaHCO₃/Na₂CO₃ buffer mixture at room temperature for 5–6 h to afford Alexa488 labeled or Fam and Tamra labeled donor probes. Unreacted dye derivatives were removed by size exclusion chromatography on a PD-10 column (Amersham Life Sciences, Piscataway, NJ). After desalting with an OPC cartridge (ABI, Foster City, CA), the products

Table 1. Binary probe sequences

Sequence name	Sequence	Molar mass (g/mol)	
		Calcd	Found
A1	5'-Cy5 GUA UGU UUC ACU GGA UGA-3'	6485	6489
B4	5'-AAG UUG AUC AAG UdT(Alexa488)G GU-3'	6337	6330
B6	5'-AAG UUG AUC AAG dT(Fam)UG GUTamra-3'	6807	6807
Target region from full length sensorin mRNA	5'-GTC ATC CAG TGA AAC ATA C AGC AC CAA CTT GAT CAA CTT G -3'	—	—

were dried under vacuum. For acceptor probe synthesis, 5'-amino group modified 2'-methoxy RNA was synthesized using 5'-amino-modifier C3 TFA as a final coupling monomer. After cleavage and deprotection, the crude 5'-Cy5 labeled oligonucleotides were obtained by coupling with Cy5 NHS ester under similar conditions as above. The products were purified by reverse-phase HPLC (Waters system containing Waters Delta 600 controller, Rheodyne 7725i injector and 2996 photodiode array detector, Milford, MA) using a C-18 reverse column (Xterra MS C18, 4.6 mm × 50 mm) at a flow rate of 0.5 ml/min and with a linear gradient of 12–34.5% of methanol in A over 40 min (A: 8.6 mM triethylammonium and 100 mM hexafluoroisopropyl alcohol aqueous solution, pH 8.1). The elution was detected at 260, 490, 580, and 650 nm. Fractions containing the desired product were collected, evaporated to dryness under vacuum, and characterized by MALDI-TOF mass spectrometry (Table 1).

BP sequences were designed to target a region of sensorin mRNA from neurons of *Aplysia californica*. The regions of sensorin mRNA were selected to possess limited secondary structure in order to improve the chance of hybridization of the probes. Details on the modeling of sensorin mRNA secondary structure as well as its synthesis have been reported elsewhere.¹³

The concentrations of the BPs were determined by UV–vis spectrometry on a Lambda 40 UV–vis spectrophotometer (Perkin Elmer, Norwalk, CT, USA). Steady-state and polarization measurements were performed on a SPEX FL3-22 Fluorolog-3 spectrometer (J. Y. Horiba, Edison, NJ, USA) in quartz cuvettes of 0.4 mm path length. In a typical experiment, 0.5 μL of target mRNA (10 μM) was added to 250 μL of a solution of 0.02 μM B4 or B6 and 0.1 μM A1 in 10 mM Tris–HCl, 400 mM NaCl, pH 7.5 (hybridization time=1 h, room temperature). The spectra were corrected for spectral efficiencies of the monochromator and PMT.

Glan Thompson polarizers were used for fluorescence depolarization measurements. The polarization values (*P*) for the individual dye components and the energy transfer components were determined by exciting one dye with linear polarized light and analyzing the depolarization of the fluorescence at different wavelengths for the two fluorophores.

Time-resolved fluorescence measurements utilized a Hamamatsu streak camera, Model C4334, optically coupled to a charge-coupled-device (CCD) array detector. This system

allowed the measurements of both the emission decay and time-resolved emission spectra. For this latter study a Chromex 205i imaging spectrometer was used. The excitation source for these studies was an all-solid state laser system from Spectra Physics, which incorporates the following components: a diode-pumped Millennia V-P laser for exciting mode-locked lasing from a Tsunami (Model 3941-M1S) Ti-sapphire laser, which in turn was amplified by a Spitfire regenerative amplifier with a Merlin regenerative pump source. Tunable, femtosecond radiation was acquired through the use of an optical parametric amplifier (OPA-800P) in combination with harmonic generation and sum-difference packages. The tunable laser pulses were of ca. 150 fs in duration at a repetition rate of 1 kHz. The ultimate time resolution that we have been able to attain with this system, using the Hamamatsu U4290 fluorescence analysis software, was estimated to be ~ 10 ps.

3. Results and discussion

3.1. Binary probe design

The design of BPs is based on the spectroscopic characteristics of the fluorophores used as reporters and on physical considerations, such as the distance and orientation of the dyes relative to one another. These factors were carefully selected to maximize the transfer of energy from the donor to the acceptor fluorophore. Förster's theory states that the efficiency (E) of FRET is expressed by Eq. 1:

$$E = \frac{R_0^6}{R_0^6 + R^6} \quad (1)$$

where R is the distance between the fluorophores and R_0 (Förster distance) is the distance at which half the donor excitation is transferred to the acceptor. The parameter R_0 is described by Eq. 2:

$$R_0^6 = \frac{9000(\ln 10)\kappa^2\phi J}{128\pi^5 n^4 N_{Av}} \quad (2)$$

where n is the refraction index of the medium, N_{Av} is the Avogadro's number, κ^2 is the orientation factor (usually used as 2/3 for free molecules in solution), and J is the spectral overlap constant given by Eq. 3:

$$J = \int_0^{\infty} f_D(\lambda)\varepsilon_A(\lambda)\lambda^4 d\lambda \quad (3)$$

where $f_D(\lambda)$ is the fluorescence spectrum of the donor and $\varepsilon_A(\lambda)$ is the absorption spectrum of the acceptor (in extinction coefficient units). Finally, the experimental FRET efficiency can be calculated using Eq. 4:

$$E = 1 - \frac{F_{DA}}{F_D} \quad (4)$$

where F_D and F_{DA} are the fluorescence of the donor in the absence and presence of acceptor, respectively.

The design of the three-dye system (**BP-3d**) requires a good spectral overlap between the primary donor and the primary acceptor/secondary donor, and subsequently a good spectral overlap between the primary acceptor/secondary donor and the secondary acceptor. We chose the fluorophores combination Fam–Tamra–Cy5 for the synthesis of **BP-3d**. The strategy for the selection of these dyes was to maximize the overlap integral (J , Eq. 3) for each FRET step. The sequence and the positioning of the dyes in **BP-3d** are shown in Table 1 (sequences A1 and B6). The calculated J constants were $3.65 \times 10^{-13} \text{ cm}^6 \text{ mol}^{-1}$ for Fam–Tamra, and $8.56 \times 10^{-13} \text{ cm}^6 \text{ mol}^{-1}$ for Tamra–Cy5, which represent good spectral overlaps.

The two-dye binary probe (**BP-2d**) is composed of an energy donor (Alexa488) and an energy acceptor (Cy5) with largely separated excitation profiles (7 nucleotides spacer between Alexa488 and Cy5) and is composed of sequences A1 and B4 (Table 1); λ_{exc} (Alexa488)=488 nm while λ_{exc} (Cy5)=647 nm. This spectral separation greatly reduces direct excitation of the acceptor Cy5 when the donor fluorophore is excited at 488 nm. These probes are designed such that when the BPs hybridize to target mRNA, Alexa488 and Cy5 move close to one another, and energy is transferred from Alexa to Cy5. Thus, excitation at 488 nm should produce a strong emission from Alexa488 at 515 nm in the absence of target and a strong emission from Cy5 at 667 nm in the presence of target. This large 'Stokes' shift' not only avoids direct excitation of the Cy5, but also minimizes the overlap between Alexa488 and Cy5 emission spectra. For microscopic imaging, this allows the use of bandpass filters with a wider spectral bandpass of the two detection channels; such filtering enhances the signal intensity significantly. As was mentioned before, at first sight Alexa488 and Cy5 do not seem to be a good pair for FRET studies due to the apparent poor overlap between the Alexa488 emission spectrum and the Cy5 absorption spectrum. However, as discussed above, the main factor governing FRET is the distance dependency between the fluorophores ($k_{FRET} \sim 1/R^6$);³³ therefore, even with a poor spectral overlap, if the fluorophores are close enough to each other a relatively high FRET is possible. Furthermore, the value of J (Eq. 3) is dependent on the absorption spectrum of the acceptor expressed in extinction coefficient units, which means that the spectral overlap is larger when the acceptor is a stronger light absorber. Since Cy5 possesses large extinction coefficients (e.g., $250,000 \text{ M}^{-1} \text{ cm}^{-1}$ at 646 nm)³⁴ the J value for the Alexa488–Cy5 pair is $1.34 \times 10^{-13} \text{ cm}^6 \text{ mol}^{-1}$.

3.2. Steady-state fluorescence characterization

With the purpose of studying FRET in the BP, steady-state fluorescence measurements were conducted. Figure 2 shows the steady-state fluorescence spectra of **BP-3d** with three bands centered at 518 nm, 581 nm, and 667 nm corresponding to the emission of Fam, Tamra, and Cy5, respectively (Fig. 2a). The positioning of Fam and Tamra within the same BP probe sequence has the purpose of creating efficient FRET from Fam to Tamra.³⁵ The spectrum of **BP-3d** before adding target sensorin mRNA shows mainly fluorescence from Tamra (581 nm) with very little fluorescence coming from Cy5. This high FRET efficiency is consistent with the high J value ($8.56 \times 10^{-13} \text{ cm}^6 \text{ mol}^{-1}$) and the close

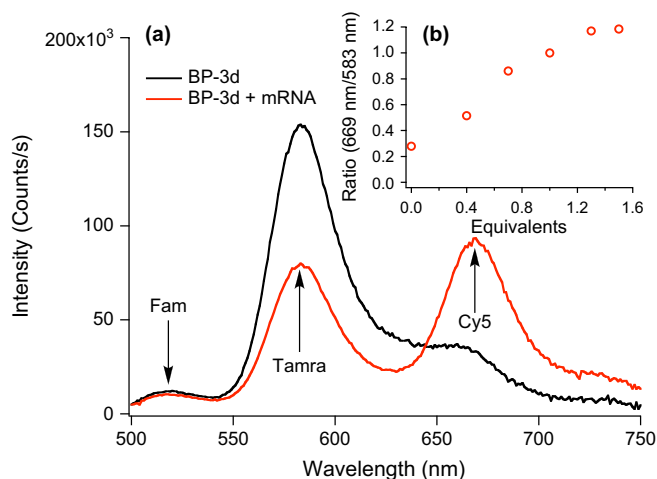


Figure 2. Steady-state fluorescence spectra of **BP-3d** ($B_6=0.02 \mu\text{M}$ and $A_1=0.1 \mu\text{M}$) in the absence (—) and presence of (—) mRNA target ($0.026 \mu\text{M}$) (a). Ratiometric intensity (Cy5/Tamra) in the presence of different amount of sensorin mRNA (b).

spacing of the two fluorophores. Hybridization of the two components of **BP-3d** to target mRNA brings together the donor and the acceptors and produces an increase in the fluorescence of Cy5. Under this scheme, Fam works as an antenna that collects the energy of absorbed photons and transfers them to Tamra; the latter fluorophore acts as a relay, or ‘energy bridge’ channeling the energy received from Fam to Cy5.³¹ This energy transfer cascade allows the coupling of three different fluorophores, resulting in a strong emission of the final energy acceptor (Cy5). The use of a relay fluorophore (Tamra) allows for a large energy separation between the primary energy donor (Fam) and the final energy acceptor (Cy5), preventing its direct excitation and increasing the amount of energy reaching Cy5. Figure 2b (inset) shows the fluorescence intensity ratio of **BP-3d** in the presence of different concentrations of sensorin mRNA. As was expected, the intensity ratio increases with the addition of target, showing a fairly linear behavior up to 1.3 equiv of mRNA. The energy transfer efficiency calculated from Eq. 4 shows ca. 47% FRET between Tamra and Cy5. Although this experimental FRET efficiency seems to be low, it is necessary to consider all the factors affecting FRET. First, the precise experimental determination of FRET efficiencies requires that all the acceptor fluorophores in the ensemble stay at FRET distance from their donors. In the case of binary probes, FRET only occurs when both probe sequences hybridize to adjacent regions of the same mRNA molecule. Unbound acceptor or donor results in unquenched emission of the donor fluorophore and an error in the determination of the FRET efficiency. Second, the fluorescence spectrum of Tamra tails into the spectral region of Cy5 fluorescence, which decreases the S/B ratio. Third, it was assumed that the orientation factor is 0.667; although this is true for random dipoles in solution media, organic fluorophores can become immobilized on the oligonucleotide macromolecule changing the value of κ^2 . Fourth, and maybe most importantly, the secondary structure of the mRNA molecule can influence the distance between the fluorophores. Because of the strong dependency of the FRET efficiency with the distance, an enlarged interfluorophore distance may decrease the FRET.

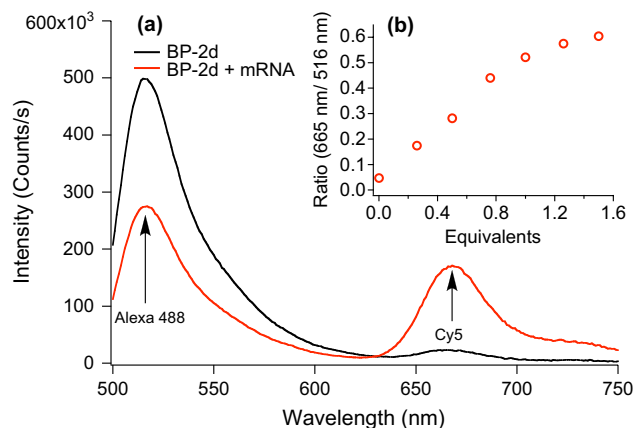


Figure 3. Steady-state fluorescence spectra of **BP-2d** ($B_4=0.02 \mu\text{M}$ and $A_1=0.1 \mu\text{M}$) in the absence (—) and presence of (—) target mRNA ($0.024 \mu\text{M}$) (a). Ratiometric intensity (Cy5/Alexa488) in the presence of different amount of mRNA (b).

The steady-state fluorescence analysis of the two-dye binary probe, **BP-2d**, is shown in Figure 3. Excitation of **BP-2d** at 488 nm in the absence of target mRNA results in a strong fluorescence from Alexa488 while only a very small fluorescence is seen from Cy5. This is in contrast with other combinations of fluorophores where the acceptor dyes fluoresce due to direct excitation.^{11,30} Another advantage of the **BP-2d** system is that the donor–acceptor emission profiles are widely spectrally separated, resulting in a large ‘Stokes’ shift’ and avoiding fluorescence overlap, which increases the sensitivity of the detection of the hybridization event. Addition of target mRNA causes hybridization of the probes to mRNA bringing together Alexa488 and Cy5. Consequently, the fluorescence signal at 515 nm decreases and the fluorescence signal at 667 nm increases due to FRET from Alexa488 to Cy5 (Fig. 3a). The intensity ratio in the presence of different amounts of mRNA is shown in Figure 3b (inset), displaying a fairly linear increase with the addition of mRNA up to 1.3 equiv. The experimental FRET efficiency calculated using Eq. 4 is 45%. Higher efficiencies might be expected however, this situation can also be explained by different factors such as free donor or acceptor molecules not bound to mRNA that do not contribute to FRET, or to an enlarged interfluorophore distance, induced by interaction with the mRNA target.

Previous studies by Tsuji et al. also present the use of dyes with widely spaced emission profiles for DNA detection.^{12,27} In those experiments the researchers used Bodipy493–Cy5 FRET pair to construct their BP obtaining similar results to ours. In our design we decided to use Alexa488 due to its high fluorescence quantum yield (0.94).³⁴ Furthermore, the Alexa488 emission spectrum is shifted to longer wavelengths than in the case of Bodipy493, providing a better overlap integral (J) and promoting more efficient FRET.

3.3. Time-resolved spectroscopic characterization

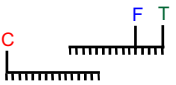
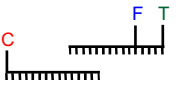
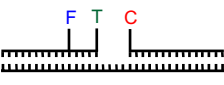
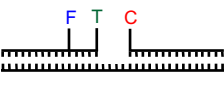
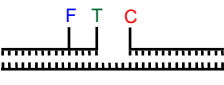
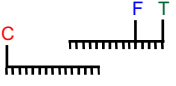
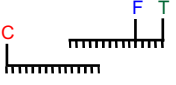
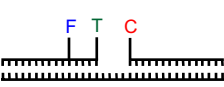
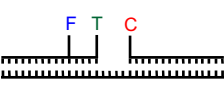
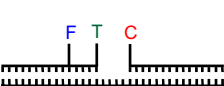
FRET dynamics of the BPs were studied using picosecond time-resolved spectroscopy. The system consists of a Ti–sapphire laser as excitation source (488 nm, 150 fs pulse)

together with a streak camera detection system coupled with a spectrograph, which allows the simultaneous collection of fluorescence decay dynamics and time-resolved fluorescence spectra. Table 2 presents some photophysical parameters collected for **BP-3d**. The lifetimes are derived from a biexponential fit of the fluorescence decays. In general, upon addition of target mRNA, the lifetimes of both Fam and Tamra decrease, consistent with FRET from these dyes to Cy5. This FRET process is triggered by the hybridization of probe sequences to adjacent sites of sensorin mRNA. The decrease in the fluorescence lifetime of Fam suggests that even when most of its energy is transferred to Tamra, after hybridization of the probe to target mRNA, Fam is still able to transfer some of its energy to Cy5. This result is consistent with previous studies of dyes covalently linked to a single DNA strand and with steady-state data from **BP-2d** where fluorescein transfers its energy to Cy5 when the probe is hybridized to mRNA.³¹ Direct excitation of Cy5 with and without target results in fairly similar lifetimes, indicating that the decay dynamics of this dye are not affected by hybridization of the probe to mRNA.

The fluorescence dynamics of **BP-2d** are shown in Figure 4. Excitation of Alexa in the absence of target shows a fluorescence decay dominated by a 3.0 ns component (Table 3). Addition of the target is followed by hybridization with the BP resulting in energy transfer from Alexa to Cy5, which is demonstrated by the more rapid decay dynamics of Alexa, especially its fast component. Furthermore, the rise of the acceptor fluorescence (Cy5) is observable. Both, the decay of Alexa488 fluorescence (fast component) and the growth of the Cy5 fluorescence, occur on a much longer time scale compared to the FRET pair Fam–Tamra in **BP-3d**. Because the overlap integral (J) is smaller for the FRET pair Alexa–Cy5 compared to Fam–Tamra, the energy transfer occurs more slowly. However, the energy transfer is fast enough to generate sufficient FRET. Previous studies on single stranded DNA with Fam and Cy5 covalently attached showed similar slow FRET dynamics.³¹

A more detailed analysis of the decay dynamics is desirable in order to extract more exact FRET parameters, however, such analysis becomes cumbersome due to the complexity of the system. Different quenching mechanisms and multiple

Table 2. Lifetime and polarization values of **BP-3d**

BP-3d	Excitation/emission	Excitation/emission, nm	τ_1 , ns (contribution %)	τ_2 , ns (contribution %)	P
	Fam/Fam	488/515	3.16 ^c (82)	0.20 ^c (18)	— ^a
	Fam/Tamra	488/559	2.91 ^c (66)	0.62 ^c (34)	0.07
	Fam/Fam	488/515	2.65 ^c (46)	0.03 ^c (54)	— ^a
	Fam/Tamra	488/559	2.57 ^c (79)	0.07 ^c (21)	0.33
	Fam/Cy5	488/667	1.77 ^c (17)	0.87 ^c (83)	0.05
	Tamra/Tamra	550/559	— ^b	— ^b	0.27
	Tamra/Cy5	550/667	— ^b	— ^b	0.29
	Tamra/Tamra	550/559	— ^b	— ^b	0.32
	Tamra/Cy5	550/667	— ^b	— ^b	0.26
	Cy5/Cy5	650/667	1.7 ^c (66)	0.2 ^c (34)	0.31
	Cy5/Cy5	650/667	1.9 ^c (72)	0.1 ^c (28)	0.40

^a The fluorescence intensity of Fam is too weak to measure reliable polarization values.

^b Not determined.

^c Uncertainty ca. $\pm 10\%$.

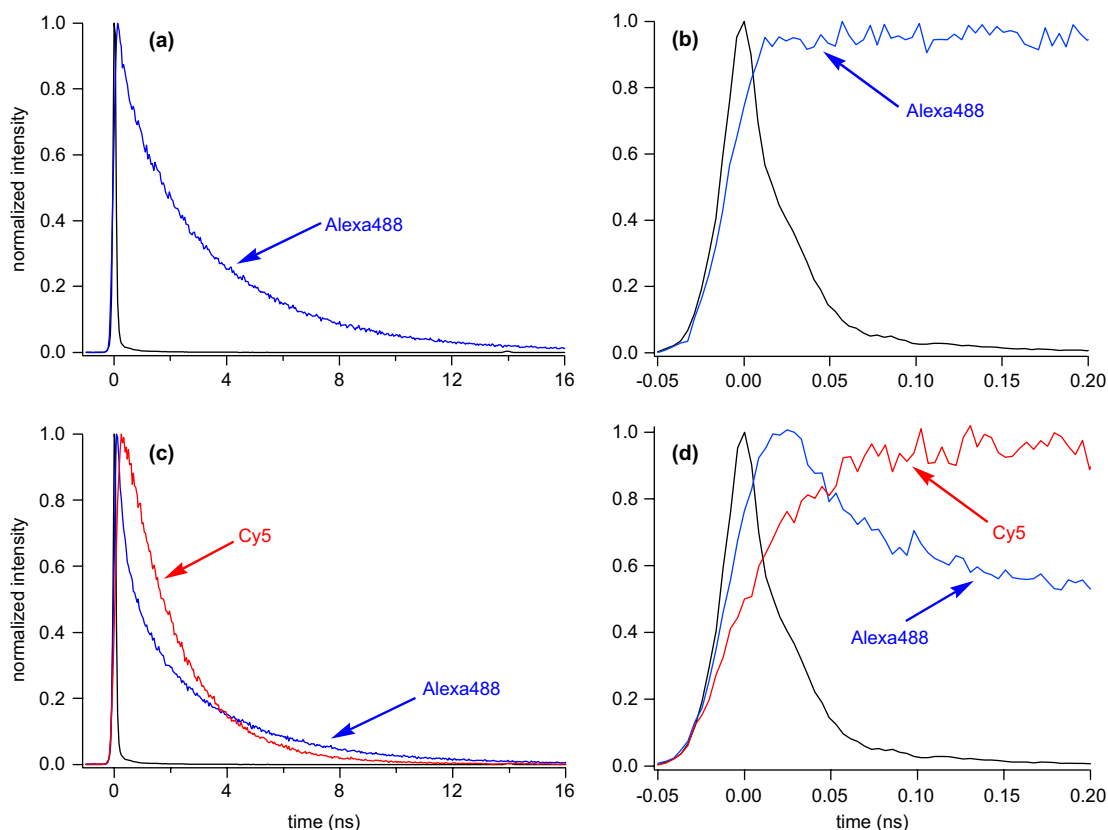


Figure 4. Time decay profiles for **BP-2d** ($B_4=0.02 \mu\text{M}$ and $A_1=0.1 \mu\text{M}$) in the absence (a) and (b), and in the presence of target mRNA ($0.024 \mu\text{M}$) (c) and (d). Alexa488 was monitored from 500–575 nm; Cy5 was monitored from 650–725 nm.

microenvironments fostered by the mRNA macromolecule make the identification of exponential components and appropriate models for the analysis a challenging task.¹¹ Despite this, however, the biexponential model used provides a way to withdraw qualitative conclusions from the data.

As stated previously, FRET has the effect of reducing the lifetime of the short decay component of Alexa488 (Fig. 4c and d). Because Cy5 is not being quenched by FRET, and due to its delayed emission, Cy5 fluorescence decays slower than Alexa488 for the first 3 ns after the pulse.

Table 3. Lifetime and polarization values of **BP-2d**

BP-2d	Excitation/emission	τ_1 , ns (contribution %)	τ_2 , ns (contribution %)	P
	Alexa/Alexa	3.2 ^c (87)	0.7 ^c (11)	0.11
	Alexa/Cy5	— ^a	— ^a	— ^a
	Alexa/Alexa	3.1 ^c (84)	0.4 ^c (16)	0.13
	Alexa/Cy5	2.1 ^c (69)	1.3 ^c (31)	-0.03 ^b
	Cy5/Cy5	1.8 ^c (71)	0.9 ^c (29)	0.29
	Cy5/Cy5	2.0 ^c (86)	0.7 ^c (14)	0.37

^a The fluorescence intensity of Cy5 is too weak to obtain reliable fluorescence lifetimes and polarization values.

^b Confidence range ± 0.04 .

^c Uncertainty ca. $\pm 10\%$.

Subsequent to this initial behavior, since the lifetime of the slower component of Alexa488 is longer than that of Cy5, the signal of Cy5 decays faster and the emission of Alexa488 dominates (Fig. 4c). (This effect is not evident from the lifetimes presented in Table 3.) Since the aforementioned features are caused by FRET, they only occur in the presence of target mRNA (Fig. 4), which can be used to time filtering the emission to improve the S/B.

Time-resolved emission spectra (TRES) of **BP-2d** were obtained by integrating the emission signal for different time windows. Figure 5 shows the TRES for **BP-2d** integrating from 0.47 to 1.47 ns from the excitation pulse (Fig. 5b) as compared to a larger time window (0–20 ns; Fig. 5a); the larger time window spectrum is equivalent to the steady-state spectrum. The TRES for **BP-2d** in the presence of mRNA target integrating from 0.47 to 1.47 ns from the excitation pulse (Fig. 5) shows an increase in the Cy5/Alexa ratio from 0.82 (20 ns integration window) to 1.2 (1 ns integration window). This ratiometric increase, as suggested above, is due to the delayed emission of Cy5 caused by the slow FRET process and to the shorter-lived Alexa488 emission at these early times after excitation. We deduce that the Cy5/Alexa488 intensity ratio decreases using larger integration windows (20 ns) because the lifetime of Cy5 is shorter than that of Alexa488, which results, as mentioned earlier, in the Cy5 fluorescence vanishing faster than that of Alexa488. Hence, longer times favor the collection of more Alexa488 photons, leading to a decrease in the ratio. The desired situation is to obtain a spectrum where the transient emission intensity of Cy5 is larger than that of Alexa488. This situation is fulfilled approximately during the first 3 ns after the pulse. Therefore, it is possible to increase the sensitivity of **BP-2d** by time-resolving the emission profile, collecting only the first 2 ns of fluorescence emission.

3.4. Fluorescence depolarization

Further information concerning the photophysics of **BP-3d** and **BP-2d** can be obtained using fluorescence depolarization studies. The polarization values (P) for the fluorophores and FRET components for **BP-3d** and **BP-2d** are shown in

Tables 2 and 3, respectively. The P values were obtained by exciting one fluorophore with linear polarized light and analyzing the depolarization of the fluorescence at a different emission wavelength corresponding to the particular dye (donor and acceptor). The polarization value is related to the angle between the absorption and the emission dipoles in a molecule. Absorption of light occurs preferentially when the light is polarized parallel to the absorption dipole of the molecule. Likewise, emission occurs preferentially parallel to the emission dipole of the molecule, which is usually at a narrow angle from the absorption dipole in most organic molecules. An important cause of depolarization is the rotation of the fluorophore during its lifetime, which causes the reorientation of the molecules with respect to the polarized excitation light and consequently the loss of polarization of emitted photons. Therefore, short fluorescence lifetimes promote larger P values and vice versa for long lifetimes. A P value of zero represents a complete isotropic relaxation of the polarization due to total excited fluorophore reorientation.

The polarization of Tamra ($P_{\text{Tamra, Tamra}}$) in **BP-3d** when no target mRNA is present is 0.27, while the polarization increases to 0.32 in the presence of target. This increase is consistent with the decrease in fluorescence lifetime (Table 2), which reduces the depolarizing effect of molecular rotation. Another contributing factor can be the increase in the rotational correlational time of the probe when bound to the mRNA macromolecule. Depolarization values can also be used to study FRET. The polarization value of Cy5 when excited directly ($P_{\text{Cy5, Cy5}}$) in **BP-3d** and in the presence of target is 0.40, but is reduced to 0.26 when Tamra is excited ($P_{\text{Tamra, Cy5}}$) and 0.05 when the excitation occurs at Fam ($P_{\text{Fam, Cy5}}$). Therefore, the polarization is partially preserved during the first FRET step, but lost in the second step.

In the case of **BP-2d**, the fluorescence of Cy5 before adding target ($P_{\text{Cy5, Cy5}}$) is 0.29 but in the presence of target the value of P increases to 0.37. Because the lifetimes of Cy5 increase from the non-hybridized to the mRNA hybridized state, the increase in the polarization is counterintuitive. However, it must be considered that mRNA is a very large molecule and upon hybridization with the probes, their rotational

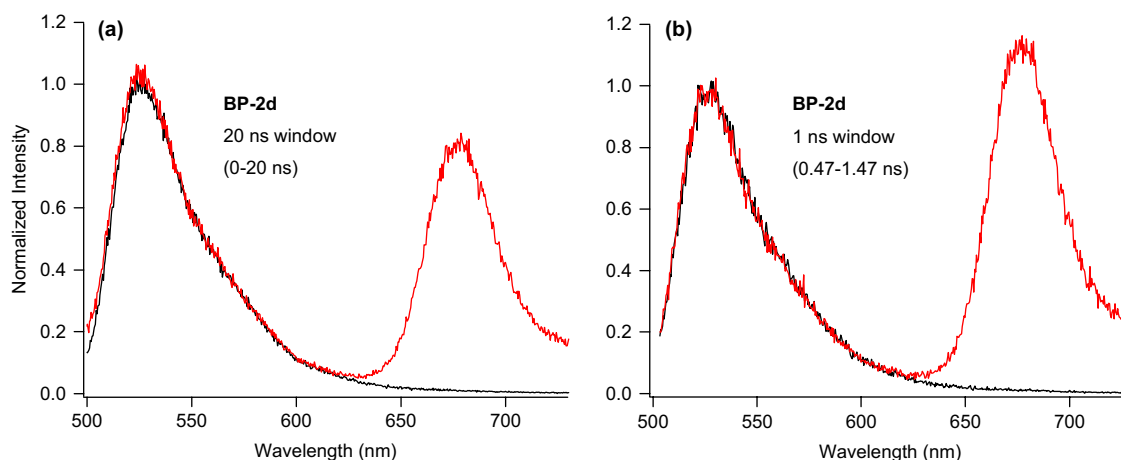


Figure 5. Time-resolved emission spectra for **BP-2d** ($B_4=0.07 \mu\text{M}$ and $A_1=0.2 \mu\text{M}$) 20 ns window, taken from 0 ns to 20 ns after the excitation pulse (a) and 1 ns window, taken from 0.47 ns to 1.47 ns after the excitation pulse (b) without (—) and with (—) target mRNA (0.07 μM).

correlation time will decrease. In this case, the decrease in rotational correlation time should compensate for the increase in fluorescence lifetime decreasing the depolarization of Cy5. This effect is also observed for **BP-3d**. The energy transfer components show the expected trend with a polarization value of 0.37 for the direct excitation of Cy5 ($P_{\text{Cy5,Cy5}}$) in the presence of target which decreases to essentially zero (Table 3) when the excitation is at Alexa488 ($P_{\text{Alexa488/Cy5}}$). One explanation for this is the slow FRET rate from Alexa488 to Cy5, which increases the fluorescence depolarization of the latter.

4. Conclusions

BP have been developed to overcome the problems of direct excitation of the acceptor and fluorescence overlap between the donor and acceptor fluorophores. **BP-3d** presents efficient energy transfer from Fam to Cy5 via a Tamra fluorophore that acts as an energy relay, accepting the energy from Fam and redirecting it to Cy5. This three-dye array is unique for binary probes, providing a framework that minimizes the direct excitation of the final acceptor Cy5, while at the same time promoting efficient energy transfer to the acceptor. **BP-2d** uses Alexa488 as the energy donor and Cy5 as acceptor. This system provides a large ‘Stokes’ shift’ and at the same time minimizes the overlap between the fluorescence emission of Alexa488 and Cy5. Steady-state fluorescence measurements showed that both **BP-3d** and **BP-2d** present good signal response in the presence of target mRNA. The fluorescence ratio for Cy5/Tamra (**BP-3d**) and Cy5/Alexa488 shows a fairly linear increase with target concentration, which suggests applications for mRNA quantification.

Picosecond time-resolved fluorescence spectroscopy showed a decrease in the lifetime of the donor fluorophores when the probes are in the presence of target mRNA. **BP-2d** showed a delayed emission in the presence of target. This delayed emission in conjunction with the decrease in the fluorescence lifetime of Alexa488 suggests the use of TRES to increase the sensitivity of the system. The Cy5/Alexa488 ratio increased from 0.82 to 1.2 when the duration of the temporally integrated spectra, as measured following the excitation pulse, was reduced from 20 ns to 1 ns, respectively. This method presents an opportunity to improve the S/B ratio of the BPs using time-resolved spectroscopy.

In conclusion, **BP-3d** and **BP-2d** illustrate interesting approaches to solve the problem of direct acceptor excitation and donor–acceptor fluorescence overlap. These approaches have direct implications for such applications of BP as SNP typing, mRNA quantification, and PCR amplification, and may offer potential opportunities for cellular imaging using these and other similarly chosen dye combinations.

Acknowledgements

This work was supported by the Center of Excellence in Genomic Science Grant P50 HG002806 from the National Institutes of Health, NSF CHE-04-15516, and by NSF CHE-04-13574. D.L.A. thanks the NSF and DoD-ARO for

support of this work, in part, through the following awards: (1) the NSF-IGERT Program, under Grant no. DGE-9972892; (2) the NSF-MRSEC Program, under Grant no. DMR-0213574; and (3) DoD-ARO, under Cooperative Agreement DAAD19-01-1-0759.

References and notes

- Fahrer, A. M.; Bazan, J. F.; Ppathanasiou, P.; Nelms, K. A.; Goodnow, C. C. *Nature (London)* **2001**, *409*, 836–838.
- Hawley, R. S.; Mori, C. A. *The Human Genome: A User's Guide*, 2nd ed.; Harcourt/Academic: Burlington, MA, 1999; pp 285–304.
- Nestler, E. J.; Landsman, D. *Nature (London)* **2001**, *409*, 834–835.
- Li, W.-H.; Gu, Z.; Wang, H.; Nekrutenko, A. *Nature (London)* **2001**, *409*, 847–849.
- Tyagi, S.; Kramer, F. R. *Nat. Biotechnol.* **1996**, *14*, 303–308.
- Tan, W.; Fang, X.; Li, J.; Liu, X. *Chem.—Eur. J.* **2000**, *6*, 1107–1111.
- Tan, W.; Wang, K.; Drake, T. J. *Curr. Opin. Chem. Biol.* **2004**, *8*, 547–553.
- Antony, T.; Subramaniam, V. J. *Biomol. Struct. Dyn.* **2001**, *19*, 497–504.
- Cardullo, R. A.; Agrawal, S.; Flores, C.; Zamecnik, P. C.; Wolf, D. E. *Proc. Natl. Acad. Sci. U.S.A.* **1988**, *85*, 8790–8794.
- Marras, S. A. E.; Tyagi, S.; Kramer, F. R. *Clin. Chim. Acta* **2006**, *363*, 48–60.
- Mergny, J.-L.; Botorine, A. S.; Garestier, T.; Belloc, F.; Rougée, M.; Bulychev, N. V.; Koshkin, A. A.; Bourson, J.; Lebedev, A. V.; Valeur, B.; Thuong, N. T.; Hélène, C. *Nucleic Acids Res.* **1994**, *22*, 920–928.
- Sei-lida, Y.; Koshimoto, H.; Kondo, S.; Tsuji, A. *Nucleic Acids Res.* **2000**, *28*, e59.
- Martí, A. A.; Li, X.; Jockusch, S.; Li, Z.; Raveendra, B.; Kalachikov, S.; Russo, J. J.; Morozova, I.; Puthanveetil, S. V.; Ju, J.; Turro, N. J. *Nucleic Acids Res.* **2006**, *34*, 3161–3168.
- Xu, Y.; Karalkar, N. B.; Kool, E. T. *Nat. Biotechnol.* **2001**, *19*, 148–152.
- Sando, S.; Kool, E. T. *J. Am. Chem. Soc.* **2002**, *124*, 2096–2097.
- Abe, H.; Kool, E. T. *J. Am. Chem. Soc.* **2004**, *126*.
- Thelwell, N.; Millington, S.; Solinas, A.; Booth, J.; Brown, T. *Nucleic Acids Res.* **2000**, *28*, 3752–3761.
- Holland, P. M.; Abramson, R. D.; Watson, R.; Gelfand, D. H. *Proc. Natl. Acad. Sci. U.S.A.* **1991**, *88*, 7276–7280.
- Kandimalla, E. R.; Agrawal, S. *Bioorg. Med. Chem.* **2000**, *8*, 1911–1916.
- Frutos, A. G.; Pal, S.; Quesada, M.; Lahiri, J. J. *J. Am. Chem. Soc.* **2002**, *124*, 2396–2397.
- Tyagi, S.; Bratu, D. P.; Kramer, F. R. *Nat. Biotechnol.* **1998**, *16*, 49–53.
- Bonnet, G.; Tyagi, S.; Libchaber, A.; Kramer, F. R. *Proc. Natl. Acad. Sci. U.S.A.* **1999**, *96*, 6171–6176.
- Tyagi, S.; Marras, S. A. E.; Kramer, F. R. *Nat. Biotechnol.* **2000**, *18*, 1191–1196.
- Bonnet, G.; Krichevsky, O.; Libchaber, A. *Proc. Natl. Acad. Sci. U.S.A.* **1998**, *95*, 8602–8606.
- Tanke, H. J.; Dirks, R. W.; Raap, T. *Curr. Opin. Biotechnol.* **2005**, *16*, 49–54.
- Santangelo, P. J.; Nix, B.; Tsourkas, A.; Bao, G. *Nucleic Acids Res.* **2004**, *32*, e57.

27. Tsuji, A.; Koshimoto, H.; Sato, Y.; Hirano, M.; Sei-lida, Y.; Kondo, S.; Ishibashi, K. *Biophys. J.* **2000**, *78*, 3260–3274.
28. Tsourkas, A.; Behlke, M. A.; Xu, Y.; Bao, G. *Anal. Chem.* **2003**, *75*, 3697–3703.
29. Rosmarin, D.; Pei, Z.; Blaser, M. J.; Tyagi, S. U.S. Patent & Trademark Office: 20060040275, 2006; pp 1–14.
30. Jockusch, S.; Martí, A. A.; Turro, N. J.; Li, Z.; Li, X.; Ju, J.; Stevens, N.; Akins, D. L. *Photochem. Photobiol. Sci.* **2006**, *5*, 493–498.
31. Tong, A. K.; Jockusch, S.; Li, Z.; Zhu, H.-R.; Akins, D. L.; Turro, N. J.; Ju, J. *J. Am. Chem. Soc.* **2001**, *123*, 12923–12924.
32. Van Der Meer, B. W.; Coker, G., III; Chen, S. S.-Y. *Resonance Energy Transfer: Theory and Data*; VCH: New York, NY, 1994; pp 5–33.
33. Lakowicz, J. R. *Principles of Fluorescence Spectroscopy*, 2nd ed.; Kluwer Academic/Plenum: New York, NY, 1999; pp 368–394.
34. McNamara, G.; Difilippantonio, M. J.; Ried, T. *Microscopy and Image Analysis*; Wiley: New York, NY, 2005; Vol. 4, pp 1–33.
35. Li, X.; Li, Z.; Martí, A. A.; Jockusch, S.; Stevens, N.; Akins, D. L.; Turro, N. J.; Ju, J. *Photochem. Photobiol. Sci.* **2006**, *5*, 896–902.